ATF4 regulates mitochondrial dysfunction, mitophagy, and autophagy, contributing to corneal endothelial apoptosis under chronic ER stress in Fuchs' dystrophy.

Saba Qureshi[1], Stephanie Lee[1], Lukas Ritzer[1], Stefan Y. Kim[1], William Steidl[1], Gayle Joliet Krest[2], Anisha Kasi[1], Varun Kumar[1,3] *

[1]Eye and Vision Research Institute, Department of Ophthalmology, Icahn School of Medicine at Mount Sinai, New York, New York, USA.

[2]Columbia University, New York, USA.

[3]Department of Pharmacological Sciences, Icahn School of Medicine at Mount Sinai, New York, New York, USA.

*Correspondence: Varun Kumar, Icahn School of Medicine at Mount Sinai, 1 Gustave L. Levy Pl, New York, NY 10029, USA; varun.kumar@mssm.edu

Keyword: ATF4, mitochondrial stress, mitophagy, autophagy, ER stress, cell survival

Abstract:

Purpose: Endoplasmic reticulum (ER) stress, mitochondrial dysfunction, mitophagy/autophagy are known to contribute independently to corneal endothelial (CE) apoptosis in Fuchs' endothelial corneal dystrophy (FECD). However, the role of a well-studied specific ER stress pathway (PERK-ATF4-CHOP) in regulating mitochondrial dysfunction, mitophagy/autophagy, and apoptosis is unknown. The purpose of this study is to explore the role of ATF4 in regulating mitochondrial dysfunction and mitophagy/autophagy, leading to CEnC apoptosis in FECD.

Methods: Human corneal endothelial cell line (HCEnC-21T), Fuchs' corneal endothelial cell line (F35T), and primary human corneal endothelial cells were treated with ER stressor tunicamycin (0.01, 0.1, 1, 10 μg/mL) for 24 and/or 48 hours. ATF4 siRNA was used to knock down ATF4 in 21T cell line and primary corneal endothelial cells. Cell viability was measured using an MTT assay (10 μg/mL tunicamycin for 24 hours). Mitochondrial bioenergetics was analyzed by measuring mitochondria membrane potential (MMP) loss using TMRE assay and ATP production using mitochondrial complex V assay kit at 48 hours post tunicamycin. Mitochondrial-mediated intrinsic apoptotic pathway proteins, mitophagy, and autophagy marker proteins were analyzed using Western blotting (10 μg/mL tunicamycin for 24 hours). ATF4 +/- and ATF4 +/+ mice were irradiated with UVA to assess pro-apoptotic ER stress and corneal endothelial cell death *in vivo.*

Results: F35T cell line had a significantly increased expression of ER stress pathway molecules (eIF2α, ATF4, CHOP) and mitochondrial-mediated intrinsic apoptotic molecules (cleaved PARP, caspase 9, caspase 3) along with mitochondrial fragmentation compared to 21T cells at the baseline, which further increased after treatment with tunicamycin. Mitochondrial membrane potential also significantly decreased in F35T compared to 21T after tunicamycin. ATF4 knockdown after tunicamycin significantly attenuated pro-apoptotic ER and mitochondrial stress molecules, rescued MMP loss, and reduced mitochondrial fragmentation in the 21T cell line and primary corneal endothelial cells. ATF4 knockdown post tunicamycin treatment also downregulated altered/excessive Parkin-mediated mitophagy and Akt/mTOR-mediated autophagy pathway with reduction of caspases, leading to increased cellular viability. ATF4+/- mice had significantly increased CE numbers with improved cellular morphology and decreased CHOP expression compared to ATF4+/+ post-UVA.

Conclusions: Pro-apoptotic ATF4 induction under tunicamycin-induced ER stress disrupts mitochondrial bioenergetics and dynamics, leading to activation of excessive autophagy/mitophagy. ATF4-induced activation of CHOP plays a key role in switching excessive autophagy to CEnC apoptosis. This study highlights the importance of ATF4 in ER-mitochondrial crosstalk and its contribution to CEnC apoptosis in FECD.

Introduction:

Fuchs' endothelial corneal dystrophy (FECD) is a heritable degenerative disorder of the corneal endothelium that affects about 4% of people over 40 and has a higher incidence in females.[1] Proteomic analysis has demonstrated that in FECD, extracellular membrane (ECM) dysregulation leads to aberrant organization of the corneal endothelial layer and Descemet's membrane.[2] The molecular pathogenesis of FECD is an area of active research. Prior work indicates that mitochondrial dysfunction contributes to FECD development.[3,4] Other research has emphasized the importance of endoplasmic reticulum (ER) stress in promoting the pathogenesis of FECD.[5,6] While ER-mitochondrial crosstalk has been shown to play a role in the development of neurodegenerative diseases such as Parkinson's disease, Huntington's disease, amyotrophic lateral sclerosis, and Alzheimer's disease, among others[7-10], there has been significantly less research regarding the role of ER-mitochondrial crosstalk in the development of FECD.

Our lab previously demonstrated that ER stress leads to mitochondrial dysfunction and contributes to corneal endothelial (CE) apoptosis. Specifically, our lab showed that induction of ER stress in the HCEnC-21T cell line via tunicamycin led to upregulation of three ER stress pathways: PERK-eIF2α-ATF4-CHOP, ATF6, and IRE1α-XBP1.[11] There was also upregulation of the apoptotic proteins cytochrome C, cleaved caspase 9, caspase 3, Bax, and PARP, as well as downregulation of the apoptosis inhibitor Bcl-2.[11]We confirmed that this ER stress-induction in the HCEnC-21T cell line led to decreased ATP production, loss of mitochondrial membrane potential (MMP), and increased mitochondrial fragmentation, as well as upregulation of the mitochondrial fission proteins p-Drp1 and Fis1.[11] In addition, the Fuchs F35T cell line also exhibited upregulation of the ER stress proteins CHOP, XBP1, p-eIF2apha, and GRP78, when compared to the untreated HCEnC-21T cell line.[11] While our research showed upregulation of the PERK-eIF2α-ATF4-CHOP pathway, further research needs to be performed to elucidate the specific role of ATF4 (a major regulatory transcription factor of PERK-CHOP pathway) in regulating ER-mitochondrial crosstalk and its contribution to FECD pathophysiology.

ATF4 is a transcription factor that contributes to the integrated stress response (ISR), which allows eukaryotic cells to maintain homeostasis in response to cellular stresses.[12,13] This transcription factor functions to upregulate stress-response genes but can also act as a transcription repressor.[14] ATF4 aids in cellular homeostatic maintenance and organellar signaling, which could have implications for a mechanistic role of ATF4 in ER-mitochondrial crosstalk and the development of FECD and warrants further investigation. Specifically, ATF4 is upregulated in response to crosstalk between the endoplasmic reticulum (ER) and mitochondria, as research has shown that mitochondrial dysfunction can promote ER stress and, thus, upregulation of the unfolded protein response (UPR), which affects downstream transcription.[15] ATF4 is also a key player in the mitochondrial stress response through the upregulation of cytoprotective genes upon induction of mitochondrial stress.[16] ER-mitochondrial crosstalk has been shown to upregulate mitophagy upon induction of ATF4 by toxic hexavalent chromium.[17] ATF4 facilitates autophagy in the setting of ER stress by transcriptionally regulating proteins that contribute to autophagosome formation.[18] For instance, ATF4 promotes and regulates autophagy in mammalian cells in response to tunicamycin-induced ER stress.[19] ATF4 also regulates autophagy in the setting of ER stress caused by severe hypoxia by inducing transcription of the protein MAP1LC3B.[20] ATF4 has also been shown to induce autophagy in cancerous cells being targeted by chemotherapeutic agents.[21] In addition to its role in autophagy, ATF4 plays a role in apoptosis by enabling the degradation of XIAP during chronic ER stress, thus promoting cell death.[22] UV radiation can also lead to decreased ATF4 expression, which requires further investigation. Research has demonstrated that UV radiation may also play a role in the development of FECD.[23,24]

While prior research establishes the role of ATF4 in organellar crosstalk and cellular homeostasis, there is a need for research that examines the mechanistic contribution of ATF4 to FECD pathogenesis. In our lab's first publication, we discussed the crosstalk between ER and mitochondria in the corneal endothelium. In this paper, we hypothesized that ATF4 plays an important role in ER-mitochondrial crosstalk, specifically in mitochondrial stress, mitophagy, autophagy, and apoptosis in FECD. This is the first study to demonstrate differential effect on mitophagy/autophagy after ER stress induction on normal corneal endothelial and Fuchs' corneal endothelial cell lines. This study specifically investigates the role of ATF4 in mitochondrial stress and

apoptosis and examines whether knocking down ATF4 plays a role in the reversal of Parkin-mediated mitophagy and mTOR/Akt-mediated autophagy. Finally, this study examines the effect of genetic loss of ATF4 on CE viability after Ultraviolet A (UVA)-induced FECD model in vivo.

Methods:

Normal and Fuchs' cell line culture

Human corneal endothelial cell line (HCEnC-21T) (a kind gift from Ula V. Jurkunas, Harvard University) was maintained in Chen's medium containing Opti-MEM (cat no. 51985034; Thermo Fisher, Waltham, MA, USA), 8% fetal bovine serum (cat no. A3840002; Thermo Fisher), 0.1 gm calcium chloride (cat no. C7902; Sigma-Aldrich, St. Louis, MO, USA), 0.4 gm chondroitin sulfate (cat no. C9819, Sigma Aldrich), gentamycin (0.5%) (cat no. 15750078; Thermo Fisher) antibiotic-antimycotic (1%) (cat no. 15240096; Millipore Sigma, Burlington, MA, USA), 25 µL of epidermal growth factor (cat no. GF144; Thermo Fisher) 50 µg of bovine pituitary extract (cat no. 50-753-3049; Fisher Scientific). Cells were grown on a T75 flask (cat no. 156499; Thermo Fisher) coated with FNC coating mix (cat no. 0407; Athena Enzyme Systems, Baltimore, MD, USA) passaged every two or three days and maintained in an incubator containing 5% CO2 at 37°C. The culture of Fuchs' corneal endothelial dystrophy cell line 35 (F35T, 1500 CUG repeats) (a generous gift from Dr. Albert S. Jun, Johns Hopkins University) was maintained in Opti-MEM (cat no. 51985034; Thermo Fisher) supplemented with 8% fetal bovine serum, 0.1 gm calcium chloride (cat no. C7902; Sigma-Aldrich), 0.4 gm chondroitin sulfate (cat no. C9819; Sigma-Aldrich), gentamycin (0.5%) (cat no. 15750078; Thermo Fisher), antibiotic-antimycotic (1%) (cat no. 15240096; Millipore Sigma), 25 µL of epidermal growth factor (cat no. GF144; Thermo Fisher), 100 µL of nerve growth factor (cat no. 13257-019; Thermo Fisher), and 10 mg of ascorbic acid (cat no. 255564; Sigma-Aldrich). Cells were grown on a T25 flask (cat no. 156340; Thermo Fisher) coated with FNC coating mix (cat no. 0407; Athena Enzyme Systems), passaged every two or three days, and maintained in an incubator containing 5% CO_2 at 37°C.

Human primary corneal endothelial culture

We isolated corneal endothelial cells from human donor corneal tissues (Eversight, Chicago, IL, USA) and established primary cell culture. Corneas were washed with M199 medium (Gibco) supplemented with gentamycin (0.5%) and antibiotic-antimycotic (1%). The corneal endothelium layer was peeled off from Descemet's membrane (DM) and stripped into smaller pieces and placed in a tube with fetal bovine serum (15%), antibiotic-antimycotic (1%), gentamycin (0.5%) and it was incubated for 2-5 days. It was then centrifuged at 3000 rpm for 6 min at RT, the supernatant was discarded, and the cells/DM strips were rinsed with HBSS by gentle flicking, re-pelleted, added 0.02% EDTA, and incubated at 37°C for 1 h. Then the tissue/cells were passed through a glass Pasteur pipette 15-20 times gently and added 2 ml of growth medium and centrifuged at 3000 rpm for 6 min at RT, supernatant was discarded, and pellet was resuspended in 500 µL of growth medium. The primary cell culture was maintained in growth medium constituted of Opti-MEM-1 (Gibco) supplemented with 8% FBS, 5 ng/ml human recombinant EGF (Peprotech), 20 ng/ml human recombinant NGF (Peprotech), 100 µg/ml bovine pituitary extract (Biomedical tech), 0.5 mM Ascorbic acid 2-phosphate (Sigma), 200 mg/L $CaCl_2$, 0.08% chondroitin sulphate, 0.5% gentamycin, 1% antibiotic-antimycotic, passaged every 2 days and maintained in an incubator containing 5% CO_2 at 37°C.

siRNA transfection

HCEnC-21T, F35T, and primary corneal endothelial cells were transfected with silencer-select negative control siRNA (cat no. 4390846) or ATF4 siRNA (cat no. 4392420), (both Thermo Fisher Scientific, CA, USA) by using a Lipofectamine RNAi Max transfection reagent (Invitrogen, Life Technologies, CA, USA) according to manufacturer's protocol. At 48 h after transfection, the cells were subjected to different doses of tunicamycin based on needs of the different experiments.

MTT assay for cell viability

The primary corneal endothelial cells (1×10^4 cells/well) were seeded and grown in 96-well plates (cat no. 701003; Fisher Scientific). Cells were transfected with ATF4 siRNA and then treated with dimethyl sulfoxide (DMSO) (0.2%) and tunicamycin (10 µg/mL) and incubated for 24 hours. We performed MTT (3-(4,5-

dimethylthiazol-2-yl)-2-5-diphenyltetrazolium bromide) assay (cat no. V13154; Thermo Fisher) for determining cell viability after different tunicamycin treatments as per the manufacturer's protocol.

Measurement of MMP

MMP was measured using the TMRE-Mitochondrial Membrane Potential Assay Kit (ab113852; Abcam) as per the manufacturer's protocol. HCEnC-21T and F35T (1×10^4 cells/well) cells were seeded in 96-black well flat bottom plates (cat no. 3916; Corning, Inc., Corning, NY, USA) until 70% to 80% confluency, then treated with and without different concentrations of tunicamycin (0.01, 0.1, 1 and 10 µg/mL) and then incubated for 48 hours. Then fluorescence (ex/em: 549/575 nm) was measured using a plate reader (Varioskan LUX; Thermo Fisher). We also transfected primary corneal endothelial cells with ATF4 siRNA for ATF4 knockdown and assessed MMP.

Measurement of Complex V (ATP Synthase) activity for ATP production

21T Human corneal endothelial cells were seeded in 150 mm plates until 70-80% confluent, and corresponding treatments were applied to the cells for 48 hours. Post-treatment, cells were pelleted, and sample preparation, along with measurement of Complex V activity, was performed using the ATP Synthase Enzyme Activity Microplate Assay Kit as per manufacturer's protocol (cat no. ab109714; Abcam, Cambridge, UK). Absorbance was measured at OD 340 nm at 30°C using a microplate reader (Varioskan LUX; Thermo Fisher).

Transmission Electron Microscopy

HCEnC-21T and F35T (4×10^4 cells/well) were seeded in 8 well Permanox Lab-Tek Chamber Slides (cat no. 70413; Fisher Scientific), grown to 80% confluency, and treated with 10 µg/mL of tunicamycin. For the transfection experiment, HCEnC-21T was transfected with negative control siRNA or ATF4 siRNA and then treated with 10 µg/mL of tunicamycin. The protocol from our previous publication was followed.[11]

Parkin plasmid transfection

HCEnC-21T cells were transfected with 0.4 µg of YFP-Parkin using Lipofectamine RNAi Max transfection reagent (Invitrogen, Life Technologies, CA, USA) and incubated for 30 hours. Then we added DMSO and tunicamycin (20 µg/mL) for 6 hours. The cells were then fixed in PFA, permeabilized in PBS and Triton X and blocked for 1 hour (normal goat serum+ 0.1 g BSA+ Tween 20). Then we incubated with mouse anti-Cytochrome C (cat no.12963S, 1:1000; Cell Signaling) overnight at 4°C. The next day, the cells were incubated with goat anti-mouse secondary antibody (Alexa Fluor 647, cat no. 1510115 1:1000; Abcam) for 1 hour. Cells were washed with PBS and stained with DAPI and visualized on a confocal microscope.

Immunostaining

HCEnC-21T (4×10^4 cells/well) and F35T were seeded in 2, 4 or 8 well chamber slides to grow up to 70% to 80% confluency. For ATF4/Mitotracker staining, the cells were incubated with MitoTracker Deep Red FM (50 nM) (cat no. M22426; Invitrogen) for 30 minutes, then fixed with paraformaldehyde (PFA) (4%) (cat no. J19943.K2; Thermo Fisher) for 20 minutes, blocked for one hour in blocking buffer (5% normal goat serum + 0.3% Triton X-100 [cat no. X100; Millipore Sigma]) and then incubated with rabbit anti- ATF4 antibody (cat no. 11815S, 1:1000; Cell Signaling, Danvers, MA, USA) overnight at 4°C. The next day, the cells were washed with ice-cold phosphate buffer saline solution (PBS) (cat no. 10010072; Thermo Fisher) three times and incubated with goat anti-rabbit secondary antibody (Alexa Fluor 488, cat no. ab1550077, 1:1000; Abcam, Cambridge, UK) for 1 hour. Cells were washed again with cold-ice PBS and stained nuclei with DAPI (cat no. D1306; Invitrogen). Slides were visualized on a confocal microscope (Leica STED 3X; Leica, Wetzlar, Germany). We also used primary corneal endothelial cells to probe for cytochrome C and ATF4. A similar immunocytochemistry method was used for staining mitochondria by mouse anti-cytochrome C (cat no. 12963S, 1:1000; Cell Signaling) and co-incubated with rabbit anti- ATF4 antibody except for treatment (0.4% DMSO; 20 µg/mL tunicamycin for 6 hours) prior to fixation. The next day, the cells were co-incubated with goat anti-rabbit secondary antibody (Alexa Fluor 488, cat no. ab1550077) and goat anti-mouse secondary antibody (Alexa Fluor 647, cat no. ab1510115, 1:1000; Abcam) for 1 hour. Cells were washed with PBS and stained with DAPI and visualized on a confocal microscope. For transfection experiment, primary corneal endothelial cells were transfected with negative control siRNA or ATF4

siRNA. At 48 h after transfection, the cells were treated with 10 μg/mL of tunicamycin, then followed the same staining procedure for ATF4 and cytochrome c. For the human corneal tissue immunostaining, Descemet's membrane containing endothelial cells was stripped from human donor corneas and treated with DMSO (0.2%) and tunicamycin (10 μg/mL) and incubated for 24 hours. After treatment, fixation, and blocking, the tissues were then incubated with mouse anti-CHOP antibody (cat no. 2895S, 1:1000; Cell Signaling) and rabbit anti-ATF4 antibody overnight at 4°C. For quantifying $ATF4^{+}DAPI^{+}$ cells per visual field (×40 lens), 10 to 15 images were taken under each condition, and the total number of $ATF4^{+}$ $DAPI^{+}$ cells was counted and averaged. A similar procedure was followed for calculating the percentage of fragmented mitochondria using cytochrome C. Quantification was masked to reduce the experimental bias. For ZO-1 staining, a dissected mouse cornea cup was fixed with 70% ethanol for 30 min at room temperature, permeabilized with 0.2% Triton X-100 in PBS for 10 min, and then blocked with 2% bovine serum albumin (BSA)-PBS for 15 to 30 min. The cornea cup was then incubated with an anti-ZO-1 antibody (cat no. ZO1-1A12, Invitrogen) in 4% BSA-PBS at 4 °C overnight. The tissues were washed with PBS the following day and incubated with goat anti-mouse secondary antibody for 1 hour. Slides were made and imaged with confocal microscopy. In vivo CE quantification was performed using ImageJ software with the Cell Counter function to count stained cells within each visual frame. For each experimental condition, five images were analyzed, and cell counts from these images were averaged to obtain a representative cell count.

Western blot

HCEnC-21T and F35T were treated either with or without DMSO or tunicamycin (DMSO: 0.0002, 0.002, 0.02, 0.2%; tunicamycin: 0.01, 0.1, 1, 10 μg/mL) for 24 hours for analyzing ER and mitochondrial stress proteins. Primary corneal endothelial cells were transfected with ATF4 siRNA and treated with DMSO or tunicamycin (10 μg/mL) for 24 hours for analyzing autophagy markers. Cells were lysed using RIPA lysis and extraction buffer (cat no. 89900; Thermo Fisher) containing protease and phosphatase inhibitor cocktail (cat no. 78440, 1:1000; Thermo Fisher) at 24 hours and spun in a centrifuge at 10,000g for 10 minutes at 4°C. The supernatant was collected and assessed to quantify protein concentration (A53227; Thermo Fisher). For the transfection experiment, primary corneal endothelial cells were transfected with negative control siRNA or ATF4 siRNA. At 48 h after transfection, the cells were treated with 10 μg/mL of tunicamycin. Protein 30 μg mixed with appropriate LDS sample buffer (cat no. NP0007; Thermo Fisher) and reducing agent (cat no. NP0009; Thermo Fisher) was subjected to 4% to 12% sodium dodecyl sulfate-polyacrylamide gel electrophoresis (cat no. NP032; Thermo Fisher), followed by transfer to polyvinylidene difluoride membrane (cat no. 88518; Thermo Fisher) at 30 V for 90 minutes. The blots were blocked in blocking buffer (25 mM Tris, 0.15 M NaCl, 0.05% Tween 20, 5% skim milk) for one hour at room temperature and then treated with primary antibody (p-eIF2α cat no. 3597, eIF2α cat no. 5324, CHOP cat no. 2895, ATF4 cat no. 11815, GAPDH cat no. 97166, Bcl2 cat no. 4223, cleaved caspase 9 cat no. 20750, cleaved caspase 3 cat no. 9661, PARP cat no. 9532, Mfn2 cat no. 11925, PINK1 cat no. 6946, Parkin cat no. 4211, LC3A/B cat no. 12741, Tim23 cat no. 67535, LC3B cat no. 3868, VDAC cat no. 4661, P-mTOR cat no. 5536, mTOR cat no. 2983, P-Akt cat no. 4060, Akt cat no. 4691, P-AMPKα cat no. 2535, AMPKα cat no. 5831, Actin cat no. 3700; all from Cell Signaling; except Tim23 from Proteintech) overnight at 4°C. The next day, the blots were washed three to five times in TBS-Tween 20 (25 mM Tris, 0.15 M NaCl, 0.05% Tween 20) (cat no. 28360; Thermo Fisher) and HRP-conjugated secondary antibody (anti-mouse IgG cat no. 7076S, Anti-rabbit IgG cat no. 7074S; Cell Signaling) was added for one hour with similar subsequent washing. The immunoreactive bands were visualized using a Femto (cat no. 34094; Thermo Fisher) or pico chemiluminescent substrate (cat no. 34579; Thermo Fisher). The band intensity was measured and quantified using ImageJ software.

Animals: ATF4+/+, ATF4+/-, ATF4-/- mice (JAX:013072) were generated at Jackson Laboratory (Farmington, CT, USA) by embryo reconstitution and crossing with healthy wild-type-C57BL6/N mice. Monogamous pairs consisting of one male and one female ATF4+/+ and ATF4+/- mouse were crossed as per a homozygous X heterozygous breeding scheme. Litters were genotyped by TransnetYX (Cordova, TN) to identify ATF4+/+ and ATF4+/- mice. Mice were housed at the animal housing facility, Eye and Vision Research Institute (EVRI), Mount Sinai, New York, USA, in a controlled environment with constant temperature, 12-h light/dark cycle, and food and water available ad libitum. Mice were anesthetized with a combined dose of ketamine (100 mg/kg) and xylazine (20 mg/kg) administered intraperitoneally (IP). Animal studies were in accordance with the ARVO

Statement for the Use of Animals in Ophthalmic and Visual Research as well as the NIH Guide for the Care and Use of Animals and were performed at EVRI with approval from EVRI Institutional Animal Care and Use Committees IACUC.

UVA irradiation: The methods of UVA irradiation of mouse cornea were described in our earlier publication. Briefly, we created a UVA LED light source (M365LP1; Thorlabs, USA) with an emission peak of 365 nm light, 8 nm bandwidth (FWHM). Irradiance of 398 mW/cm^2 was focused down to a 4 mm diameter illumination spot onto the mouse cornea. The time of UVA exposure was adjusted to deliver the appropriate fluence (20 min 57 s for 500 J/cm^2) as measured with a thermal power sensor head (S425C, Thorlabs, USA) and energy meter console (PM100D, Thorlabs). We irradiated right eye (OD), while the contralateral eye (OS) served as untreated control and was covered with retention drapes (SpaceDrapes, Inc., USA). Mouse eyes were enucleated in sterile PBS, and corneas containing Descemet's membrane were isolated and immunostained based on experiments.

Results:

Differential activation of ER stress markers after chronic ER stress in 21T and F35T cell lines.

Engler and colleagues observed morphological changes in the endoplasmic reticulum (ER) and noted an increase in markers associated with the unfolded protein response (UPR), such as glucose-regulated protein (GRP78), eukaryotic initiation factor 2 subunit alpha (eIF2α), and CCAAT-enhancer binding protein homologous protein (CHOP), within the corneal endothelium of patients with FECD.[25] We first investigated the differential activation of ER stress related proteins in Fuchs' corneal endothelial cell line (F35T) compared to normal corneal endothelial cell line (21T). Immunoblotting data showed increased expression of CHOP, peIF2α, and ATF4 in F35T compared to 21T cell line under Tun (10 µg/mL,24 hours) **(Fig. 1A)**. This data confirms the involvement of ER stress in FECD. In our previous publication, we showed that the baseline ER stress markers were high in the F35T cell line, so here we used tunicamycin to see if it increases the response after tunicamycin. We also observed upregulated expression of ATF4 in F35T cell line compared to 21T cell line under normal physiological conditions. Immunostaining data showed a significant induction of ATF4, along with mitochondrial fragmentation (mitochondria labeled by Mitotracker staining) in F35T cell line compared to 21T cell line under normal physiological conditions **(Fig. 1B & C)**. We then used primary endothelial cells derived from human corneal tissues and observed ATF4 induction and Cytochrome C release post tunicamycin (10 µg/mL) treatment compared to DMSO (0.2%) at 24 hours **(Fig. 1D)**. To further validate the cell line data, we used corneal tissues to investigate ATF4 and CHOP expression. **Fig. 1E** demonstrated ATF4 and CHOP induction post tunicamycin (10 µg/mL) treatment in human corneal tissue ex-vivo using immunohistochemistry. These data suggest the activation of the PERK-eIF2α-CHOP pathway by tunicamycin in the human corneal endothelial cell line, as well as human corneal endothelial tissues and primary corneal cells and differential activation of ER stress proteins in Fuchs' cell line (F35T) compared to normal HCEnC-21T cell line.

Differential mitochondrial dysfunction and apoptosis induced by chronic ER stress in 21T and F35T cell lines.

ER stress is known to induce mitochondrial stress and dysfunction by initiating the loss of MMP and cytochrome C release from the mitochondria and decreased ATP production. We first investigated whether there are any baseline differences in MMP between normal and Fuchs' cell lines. There were no differences in MMP for HCEnC-21T and F35T cell lines at baseline. Still, as we induced ER stress using tunicamycin, we observed a dose-dependent decrease in MMP with 0.01, 0.1, 1, and 10 µg/mL tunicamycin at 48 hours in F35 T compared to 21T cell lines **(Fig. 2A).** We also found decreased ATP production in F35T cell line compared to 21T cell line at a basal level which further decreased on treatment with tunicamycin (10 µg/mL) at 48 hours **(Fig. 2B)**. Immunostaining data also showed increased mitochondrial fragmentation (confirmed by cytochrome C release from mitochondria) in F35T cell line compared to 21T cell line under DMSO control (0.2%) which further increased after Tun (10 ug/ml) **(Fig. 2C & D)**. We further investigated if mitochondrial dysfunction leads to apoptosis. Western blotting and its quantification data showed upregulation of cleaved PARP, caspase 3, caspase 9, and downregulation of Bcl-2 in F35T compared to 21T cell line at baseline control. Tunicamycin treatment (10 µg/mL, 24 hours) further increased cleaved Cas3 protein expression in F35T compared to 21T cell line **(Fig. 2E, F)**.

This data suggests that there is an altered mitochondrial function leading to apoptosis in F35T cell line compared to 21T cell line and ER stress induction further worsens it in both 21T as well as F35T cell line.

Differential mitophagy activation under chronic ER stress in 21T and F35T cell line.

We hypothesized that mitophagy plays a crucial role in initiating mitochondrial stress, so we checked for mitophagy markers. We found a significant upregulation of Parkin and LC3 and a downregulation of PINK1 in F35T compared to 21T at baseline **(Fig 3A, B**). There was a decreased expression of Mfn2 in F35T compared to 21T at baseline (**Fig 3A**). Moreover, LC3 and Parkin expression further increased in F35T compared to 21T under 10 µg/mL tunicamycin treatment at 24 hours **(Fig. 3A, B)**. We also found a key mitophagy marker, i.e., Parkin activation at damaged mitochondria indicated by cytochrome C release after ER stress induction with tunicamycin treatment (10 µg/mL) at 24 hours **(Fig. 3C & D)**. This immunostaining data further confirms that activation of mitophagy plays a crucial role in mitochondrial disruption upon ER stress. The data from TEM **(Fig. 3E)** showed that the untreated 21T cell line had intact mitochondria, while untreated F35T cells showed swollen, fragmented mitochondria with more vacuoles and autophagosomes, which further increased after 10 µg/mL tunicamycin at 24 hours.

ATF4 knockdown decreases pro-apoptotic ER and mitophagy stress proteins, attenuates mitochondrial fragmentation as well as increases cell viability under chronic ER stress.

ATF4 is a transcription factor, which is activated under chronic ER stress. To investigate the role of endogenous ATF4 in regulating the ER stress mediated mitochondrial dysfunction, we knocked down ATF4 expression. 21T cells were transfected with ATF4 small interfering RNA (siRNA) or control siRNA, and the efficiency of the ATF4 knockdown was verified at the protein level. ATF4 is recognized for its role as a protective factor during cellular stress. Its pro-death function has been linked to its regulation of CHOP, which is involved in triggering apoptosis in response to ER stress[26], and CHOP is indispensable for cell death in response to ER stress.[27] Mfn2, a mitochondrial fusion protein, plays a crucial role in regulating mitochondrial dynamics following stress. Tim23 is an integral inner membrane protein essential for mitochondrial import [28]and Tim23 depletion from cells results in a defect in import.[29] We observed decreased expression of CHOP along with other caspases (cleaved cas3 and 9) under ATF4 siRNA compared to control siRNA after Tun, which shows that ATF4 knockdown rescues the cell death-related molecules after chronic ER stress (**Fig 4A**). Mitochondria mass-related proteins, Mfn2 and Tim 23 increased in ATF4 siRNA compared to control siRNA after Tun (10 µg/mL, 24 hours). This data demonstrates that ATF4 regulates mitochondrial mass protein to control apoptosis (**Fig 4A**). We also investigated mitophagy markers and found that PINK1 increases and parkin decreases under ATF4 siRNA compared to control siRNA under Tun, suggesting ATF4 mediated Parkin-PINK1 modulation for mitophagy mechanism **(Fig. 4A)**. The MMP data **(Fig. 4B)** showed that the loss of MMP upon chronic ER stress gets rescued after ATF4 knockdown. Similarly, cell viability was also rescued under ATF4 knockdown compared to control siRNA after chronic ER stress as shown by MTT assay **(Fig. 4C).** The immunostaining data showed that upon ER stress with tunicamycin (10 µg/mL), ATF4 gets induced and leads to mitochondrial fragmentation as shown by cytochrome c staining in primary corneal endothelium cells. ATF4 knockdown significantly decreased % of cells with fragmented mitochondria compared to control siRNA under Tun. **(Fig. 4D & E).**

ATF4 knockdown rescues excessive mitophagy activation and autophagy under chronic ER stress

Chronic ER stress, due to the accumulation of unfolded proteins, is widely recognized for triggering caspase-mediated apoptosis via the unfolded protein response (UPR). Additionally, autophagy is associated with the ER-stress/UPR pathways.[30] However, it remains unclear whether autophagy regulates the UPR pathway and how specific UPR targets influence autophagy. Parkin and PINK1 are key regulators that control mitophagy and maintain mitochondrial homeostasis.[31] PINK1/Parkin-mediated mitophagy is typically viewed in the context of mitochondrial depolarization by facilitating the turnover of damaged mitochondria. We wanted to investigate if ATF4 regulates mitophagy via the PINK1/Parkin pathway. Thus, we isolated mitochondria from 21T cells and probed for Parkin, PINK1, and LC3. We found that upon ER stress (0.1 µg/mL tunicamycin, 24 hours), Parkin and LC3 were upregulated, and PINK1 was downregulated, suggesting mitophagy activation **(Fig. 5A).** When we knocked down ATF4, Parkin and LC3 B gets downregulated suggesting mitophagy rescue and proving that ATF4 regulates mitophagy via PINK1/Parkin mechanism. (**Fig 5A**). Cells experiencing ER stress initiate the

unfolded protein response (UPR) to prevent apoptosis and may also trigger autophagy. ATF4 serves as the primary signal for autophagy induced by ER stress, which later shifts to apoptosis due to the upregulation of CHOP. The transcription factors ATF4 and CHOP can independently or collectively induce autophagy regulatory factors. The PERK-eIF2α-ATF4 pathway initiates autophagy by activating AMPK and inhibiting mTOR activity.[32] Additionally, PERK-mediated expression of ATF4 and CHOP induces autophagy through the inhibition of mTOR activity.[33,34] So we investigated the Akt/mTOR pathway for autophagy, and we found that chronic ER stress activated excessive autophagy by activating the Akt/mTOR pathway with increased LC3 and phosphorylation of AMPKα and decreased phosphorylation of Akt and mTOR. This reverses when we knockdown ATF4, suggesting the role of ATF4 in regulating autophagy **(Fig. 5B, C).** The TEM data showed that tunicamycin led to swollen mitochondria and more autophagosomes, suggesting excessive mitophagy/autophagy under chronic ER stress. There were fewer autophagosomes with intact mitochondria in ATF4 siRNA compared to control siRNA under Tun-induced ER stress. This further suggests that ATF4 regulates autophagy/ mitophagy under chronic ER stress. **(Fig. 5D, E)**

ATF4 +/- mice have significantly decreased CHOP activation and increased corneal endothelial cell number compared to ATF4 +/+ post UVA.

We use our established UVA-induced mouse model of Fuchs' dystrophy to investigate the loss of corneal endothelial cells in ATF4+/+ and ATF4+/- mice corneas. For this, we irradiated ATF4 +/+ and ATF4 +/- mice eyes with UVA (500 J/cm^2) and observed the change in morphology of corneal endothelial (CE) cells outlined by ZO-1 immunostaining and counted mouse CE number. We found that ATF4 +/- mice corneas have a significantly increased number of corneal endothelial cells with more hexagonal morphology compared to ATF4 +/+ mice post-UVA (**Fig. 6A, B**) suggested that ATF regulation of CE viability in vivo. To investigate whether increased CE number in ATF4+/- mice also have decreased pro-apoptotic ER stress molecule, CHOP, we calculated % of CE cells with CHOP. We found a significantly increased % of CE cells with CHOP in ATF4+/+ compared to ATF4+/- mice at day 1 post-UVA with no differences in non-UVA control (**Fig. 6C, D**). This suggests that ATF4 regulates CE viability by regulating CHOP in vivo.

Discussion:

In this study, we have investigated the differential ER stress induction and mitochondrial dysfunction in HCEnC-21T and F35T cell lines under unstressed conditions and tunicamycin-induced ER stress. We have also investigated the role of ATF4 in ER stress-induced mitochondrial dysfunction and excessive autophagy in FECD. Specifically, we have demonstrated the upregulation of a well-known ER stress pathway (eIF2α/ATF4/CHOP) after tunicamycin treatment of HCEnC-21T and F35T cell line. F35T cell line had a significantly increased expression of ER stress pathway molecules (eIF2α, ATF4, CHOP) and mitochondrial-mediated intrinsic apoptotic molecules (PARP, Bcl2, cleaved caspase 9, cleaved caspase 3) along with mitochondrial fragmentation compared to 21T cells at the baseline, which further increased after treatment with tunicamycin. We observed differential activation of ER and mitochondrial stress, and we found that ATF4 gets activated, which follows the eIF2α/ATF4/CHOP pathway. ATF4 knockdown after tunicamycin treatment decreased ER and mitochondrial stress, rescued MMP loss and apoptosis, attenuated mitochondrial fragmentation, and modulated autophagy pathway (Akt/mTOR) in 21T cell line as well as primary corneal endothelial cells. Also, ATF4 +/- mice had significantly increased corneal endothelial cells compared to ATF4 +/+ mice post-UVA exposure.

ER stress and mitochondrial dysfunction have been known to contribute to CEnC apoptosis in FECD. Our study reported that tunicamycin induces ER stress, which has been supported by numerous studies related to ocular and neurodegenerative diseases.[5,35,36] We demonstrated the role of a known ER-stress pathway (eIF2α/ATF4/CHOP) in regulating mitochondrial dysfunction and apoptosis in FECD. Our study showed that ER stress induces mitochondrial dysfunction by promoting MMP loss, lowering ATP production, activation of caspase cascade via cleavage of caspase 3 and caspase 9, and also mitochondrial fragmentation due to cytochrome c release from mitochondria. This is evidenced by many studies which showed that mitochondrial dysfunction, ER stress and apoptosis is involved in Alzheimer's disease[37], ER stress-induced mitochondrial dysfunction in aged hearts[38], and ER stress-induced ROS-associated mitochondrial dysfunction leading to apoptosis.[39]

It remains unclear if the role of mitophagy is detrimental or beneficial in FECD. We demonstrated that tunicamycin-induced ER stress activated mitophagy in FECD. Previous studies have shown that the crosstalk between mitochondrial dysfunction and endoplasmic reticulum stress promoted ATF4-mediated mitophagy.[17] Studies have also revealed that parkin is transcriptionally regulated by ATF4.[15] This supports our data for mitophagy activation after ER stress. So, we investigated if ATF4 knockdown could rescue mitochondrial dysfunction and mitophagy/autophagy and/or cell death. It is known that UPR, autophagy, and mitochondria crosstalk underlies the ER stress response.[40] Our study demonstrated that when we knocked down ATF4, there is a rescue of mitochondrial dysfunction as evidenced by reversal of MMP loss and mitochondrial fragmentation. We also found rescue of cell death which suggests that ATF4 knockdown leads to cell survival via modulating excessive autophagy.

Previous studies have shown that ATF4 is the key signal for autophagy induced by ER stress and that autophagy is switched to apoptosis by subsequent CHOP upregulation. This suggests that the switchover switch between autophagy and apoptosis is located between ATF4 and CHOP in the PERK pathway.[41] This supports our study where we demonstrated that excessive autophagy is leading the corneal endothelium cells to apoptosis, but after ATF4 knockdown, there is a rescue of excessive autophagy, which also protects mitochondrial dysfunction and cell death in FECD. Our mouse model of UVA-induced ER stress in FECD demonstrated loss of corneal endothelial cells in wild-type UVA irradiated mice, while ATF4+/- mice showed rescue of cell loss post UVA irradiation. This suggested the role of ATF4 in regulating cell loss *in vivo* as well.

ER stress and mitochondrial dysfunction have been known to contribute to CEnC apoptosis in FECD. However, the role of ATF4 in regulating mitochondrial dysfunction and mitophagy/autophagy is unknown. Our study provides insight into the crosstalk between ER and mitochondria, as well as the mechanism of ATF4-mediated autophagy in FECD and the switch from autophagy to apoptosis post-ER stress. In future studies, we will explore the mechanisms involved in parkin-mediated mitophagy leading to mitochondrial dysfunction and cell loss in FECD and other ocular diseases. The findings of our study are promising, and they need to be tested on FECD animal models. We can also target ER and mitochondrial stress proteins for drug screening and provide therapeutic intervention for ocular diseases such as FECD.

Acknowledgements:

We sincerely thank Allison Sowa, Bill Janssen for electron microscopy processing and imaging at The Microscopy CoRE, Icahn School of Medicine at Mount Sinai. We also thank Ula V. Jurkunas (Schepens Eye Research Institute, Harvard University) for providing HCEnC-21T cell line and Albert Jun (Wilmer Eye Institute, John Hopkins University) for providing F35T cell line.

Funding:

Supported by NIH/NEI (4R00EY031339), Mount Sinai Seed Money, New York Eye and Ear Foundation, Sarah K de Coizart Charitable Trust/Foundation awarded to V.K. and Challenge Grant from Research to Prevent Blindness awarded to ophthalmology department.

Financial disclusures: None

References:

1. Krachmer, J.H., Purcell, J.J., Jr., Young, C.W., and Bucher, K.D. (1978). Corneal endothelial dystrophy. A study of 64 families. Arch Ophthalmol *96*, 2036-2039. 10.1001/archopht.1978.03910060424004.
2. Poulsen, E.T., Dyrlund, T.F., Runager, K., Scavenius, C., Krogager, T.P., Hojrup, P., Thogersen, I.B., Sanggaard, K.W., Vorum, H., Hjortdal, J., and Enghild, J.J. (2014). Proteomics of Fuchs' endothelial corneal dystrophy support that the extracellular matrix of Descemet's membrane is disordered. J Proteome Res *13*, 4659-4667. 10.1021/pr500252r.
3. Benischke, A.S., Vasanth, S., Miyai, T., Katikireddy, K.R., White, T., Chen, Y., Halilovic, A., Price, M., Price, F., Jr., Liton, P.B., and Jurkunas, U.V. (2017). Activation of mitophagy leads to decline in Mfn2 and loss of mitochondrial mass in Fuchs endothelial corneal dystrophy. Sci Rep *7*, 6656. 10.1038/s41598-017-06523-2.
4. Halilovic, A., Schmedt, T., Benischke, A.S., Hamill, C., Chen, Y., Santos, J.H., and Jurkunas, U.V. (2016). Menadione-Induced DNA Damage Leads to Mitochondrial Dysfunction and Fragmentation During Rosette Formation in Fuchs Endothelial Corneal Dystrophy. Antioxid Redox Signal *24*, 1072-1083. 10.1089/ars.2015.6532.
5. Okumura, N., Kitahara, M., Okuda, H., Hashimoto, K., Ueda, E., Nakahara, M., Kinoshita, S., Young, R.D., Quantock, A.J., Tourtas, T., et al. (2017). Sustained Activation of the Unfolded Protein Response Induces Cell Death in Fuchs' Endothelial Corneal Dystrophy. Invest Ophthalmol Vis Sci *58*, 3697-3707. 10.1167/iovs.16-21023.
6. Okumura, N., Hashimoto, K., Kitahara, M., Okuda, H., Ueda, E., Watanabe, K., Nakahara, M., Sato, T., Kinoshita, S., Tourtas, T., et al. (2017). Activation of TGF-beta signaling induces cell death via the unfolded protein response in Fuchs endothelial corneal dystrophy. Sci Rep *7*, 6801. 10.1038/s41598-017-06924-3.
7. Kaur, S., Sehrawat, A., Mastana, S.S., Kandimalla, R., Sharma, P.K., Bhatti, G.K., and Bhatti, J.S. (2023). Targeting calcium homeostasis and impaired inter-organelle crosstalk as a potential therapeutic approach in Parkinson's disease. Life Sci *330*, 121995. 10.1016/j.lfs.2023.121995.
8. Naia, L., Ferreira, I.L., Ferreiro, E., and Rego, A.C. (2017). Mitochondrial Ca(2+) handling in Huntington's and Alzheimer's diseases - Role of ER-mitochondria crosstalk. Biochem Biophys Res Commun *483*, 1069-1077. 10.1016/j.bbrc.2016.07.122.
9. Sakai, S., Watanabe, S., Komine, O., Sobue, A., and Yamanaka, K. (2021). Novel reporters of mitochondria-associated membranes (MAM), MAMtrackers, demonstrate MAM disruption as a common pathological feature in amyotrophic lateral sclerosis. FASEB J *35*, e21688. 10.1096/fj.202100137R.
10. Wang, X., Luo, D., and Wu, S. (2021). Molecular Dysfunctions of Mitochondria-Associated Endoplasmic Reticulum Contacts in Atherosclerosis. Oxid Med Cell Longev *2021*, 2424509. 10.1155/2021/2424509.
11. Qureshi, S., Lee, S., Steidl, W., Ritzer, L., Parise, M., Chaubal, A., and Kumar, V. (2023). Endoplasmic Reticulum Stress Disrupts Mitochondrial Bioenergetics, Dynamics and Causes Corneal Endothelial Cell Apoptosis. Invest Ophthalmol Vis Sci *64*, 18. 10.1167/iovs.64.14.18.
12. Neill, G., and Masson, G.R. (2023). A stay of execution: ATF4 regulation and potential outcomes for the integrated stress response. Front Mol Neurosci *16*, 1112253. 10.3389/fnmol.2023.1112253.
13. Pakos-Zebrucka, K., Koryga, I., Mnich, K., Ljujic, M., Samali, A., and Gorman, A.M. (2016). The integrated stress response. EMBO Rep *17*, 1374-1395. 10.15252/embr.201642195.
14. Ameri, K., and Harris, A.L. (2008). Activating transcription factor 4. Int J Biochem Cell Biol *40*, 14-21. 10.1016/j.biocel.2007.01.020.
15. Bouman, L., Schlierf, A., Lutz, A.K., Shan, J., Deinlein, A., Kast, J., Galehdar, Z., Palmisano, V., Patenge, N., Berg, D., et al. (2011). Parkin is transcriptionally regulated by ATF4: evidence for an interconnection between mitochondrial stress and ER stress. Cell Death Differ *18*, 769-782. 10.1038/cdd.2010.142.
16. Quiros, P.M., Prado, M.A., Zamboni, N., D'Amico, D., Williams, R.W., Finley, D., Gygi, S.P., and Auwerx, J. (2017). Multi-omics analysis identifies ATF4 as a key regulator of the mitochondrial stress response in mammals. J Cell Biol *216*, 2027-2045. 10.1083/jcb.201702058.
17. Dlamini, M.B., Gao, Z., Hasenbilige, Jiang, L., Geng, C., Li, Q., Shi, X., Liu, Y., and Cao, J. (2021). The crosstalk between mitochondrial dysfunction and endoplasmic reticulum stress promoted ATF4-mediated mitophagy induced by hexavalent chromium. Environ Toxicol *36*, 1162-1172. 10.1002/tox.23115.

18. B'Chir, W., Maurin, A.C., Carraro, V., Averous, J., Jousse, C., Muranishi, Y., Parry, L., Stepien, G., Fafournoux, P., and Bruhat, A. (2013). The eIF2alpha/ATF4 pathway is essential for stress-induced autophagy gene expression. Nucleic Acids Res *41*, 7683-7699. 10.1093/nar/gkt563.
19. Luhr, M., Torgersen, M.L., Szalai, P., Hashim, A., Brech, A., Staerk, J., and Engedal, N. (2019). The kinase PERK and the transcription factor ATF4 play distinct and essential roles in autophagy resulting from tunicamycin-induced ER stress. J Biol Chem *294*, 8197-8217. 10.1074/jbc.RA118.002829.
20. Rzymski, T., Milani, M., Pike, L., Buffa, F., Mellor, H.R., Winchester, L., Pires, I., Hammond, E., Ragoussis, I., and Harris, A.L. (2010). Regulation of autophagy by ATF4 in response to severe hypoxia. Oncogene *29*, 4424-4435. 10.1038/onc.2010.191.
21. Milani, M., Rzymski, T., Mellor, H.R., Pike, L., Bottini, A., Generali, D., and Harris, A.L. (2009). The role of ATF4 stabilization and autophagy in resistance of breast cancer cells treated with Bortezomib. Cancer Res *69*, 4415-4423. 10.1158/0008-5472.CAN-08-2839.
22. Hiramatsu, N., Messah, C., Han, J., LaVail, M.M., Kaufman, R.J., and Lin, J.H. (2014). Translational and posttranslational regulation of XIAP by eIF2alpha and ATF4 promotes ER stress-induced cell death during the unfolded protein response. Mol Biol Cell *25*, 1411-1420. 10.1091/mbc.E13-11-0664.
23. Bahamondes Lorca, V.A., Bastidas Mayorga, B.D., Tong, L., and Wu, S. (2021). UVB-induced eIF2alpha phosphorylation in keratinocytes depends on decreased ATF4, GADD34 and CReP expression levels. Life Sci *286*, 120044. 10.1016/j.lfs.2021.120044.
24. Liu, C., Miyajima, T., Melangath, G., Miyai, T., Vasanth, S., Deshpande, N., Kumar, V., Ong Tone, S., Gupta, R., Zhu, S., et al. (2020). Ultraviolet A light induces DNA damage and estrogen-DNA adducts in Fuchs endothelial corneal dystrophy causing females to be more affected. Proc Natl Acad Sci U S A *117*, 573-583. 10.1073/pnas.1912546116.
25. Engler, C., Kelliher, C., Spitze, A.R., Speck, C.L., Eberhart, C.G., and Jun, A.S. (2010). Unfolded protein response in fuchs endothelial corneal dystrophy: a unifying pathogenic pathway? Am J Ophthalmol *149*, 194-202 e192. 10.1016/j.ajo.2009.09.009.
26. Zinszner, H., Kuroda, M., Wang, X., Batchvarova, N., Lightfoot, R.T., Remotti, H., Stevens, J.L., and Ron, D. (1998). CHOP is implicated in programmed cell death in response to impaired function of the endoplasmic reticulum. Genes Dev *12*, 982-995. 10.1101/gad.12.7.982.
27. Armstrong, J.L., Flockhart, R., Veal, G.J., Lovat, P.E., and Redfern, C.P. (2010). Regulation of endoplasmic reticulum stress-induced cell death by ATF4 in neuroectodermal tumor cells. J Biol Chem *285*, 6091-6100. 10.1074/jbc.M109.014092.
28. Dekker, P.J., Martin, F., Maarse, A.C., Bomer, U., Muller, H., Guiard, B., Meijer, M., Rassow, J., and Pfanner, N. (1997). The Tim core complex defines the number of mitochondrial translocation contact sites and can hold arrested preproteins in the absence of matrix Hsp70-Tim44. EMBO J *16*, 5408-5419. 10.1093/emboj/16.17.5408.
29. Emtage, J.L., and Jensen, R.E. (1993). MAS6 encodes an essential inner membrane component of the yeast mitochondrial protein import pathway. J Cell Biol *122*, 1003-1012. 10.1083/jcb.122.5.1003.
30. Yorimitsu, T., and Klionsky, D.J. (2007). Endoplasmic reticulum stress: a new pathway to induce autophagy. Autophagy *3*, 160-162. 10.4161/auto.3653.
31. Swerdlow, N.S., and Wilkins, H.M. (2020). Mitophagy and the Brain. Int J Mol Sci *21*. 10.3390/ijms21249661.
32. Avivar-Valderas, A., Bobrovnikova-Marjon, E., Alan Diehl, J., Bardeesy, N., Debnath, J., and Aguirre-Ghiso, J.A. (2013). Regulation of autophagy during ECM detachment is linked to a selective inhibition of mTORC1 by PERK. Oncogene *32*, 4932-4940. 10.1038/onc.2012.512.
33. Salazar, M., Carracedo, A., Salanueva, I.J., Hernandez-Tiedra, S., Lorente, M., Egia, A., Vazquez, P., Blazquez, C., Torres, S., Garcia, S., et al. (2009). Cannabinoid action induces autophagy-mediated cell death through stimulation of ER stress in human glioma cells. J Clin Invest *119*, 1359-1372. 10.1172/jci37948.
34. Bruning, A., Rahmeh, M., and Friese, K. (2013). Nelfinavir and bortezomib inhibit mTOR activity via ATF4-mediated sestrin-2 regulation. Mol Oncol *7*, 1012-1018. 10.1016/j.molonc.2013.07.010.
35. Oda, T., Kosuge, Y., Arakawa, M., Ishige, K., and Ito, Y. (2008). Distinct mechanism of cell death is responsible for tunicamycin-induced ER stress in SK-N-SH and SH-SY5Y cells. Neurosci Res *60*, 29-39. 10.1016/j.neures.2007.09.005.
36. Li, Y., Li, H.Y., Shao, J., Zhu, L., Xie, T.H., Cai, J., Wang, W., Cai, M.X., Wang, Z.L., Yao, Y., and Wei, T.T. (2022). GRP75 Modulates Endoplasmic Reticulum-Mitochondria Coupling and Accelerates Ca(2+)-

Dependent Endothelial Cell Apoptosis in Diabetic Retinopathy. Biomolecules *12*. 10.3390/biom12121778.
37. Takuma, K., Yan, S.S., Stern, D.M., and Yamada, K. (2005). Mitochondrial dysfunction, endoplasmic reticulum stress, and apoptosis in Alzheimer's disease. J Pharmacol Sci *97*, 312-316. 10.1254/jphs.cpj04006x.
38. Chen, Q., Samidurai, A., Thompson, J., Hu, Y., Das, A., Willard, B., and Lesnefsky, E.J. (2020). Endoplasmic reticulum stress-mediated mitochondrial dysfunction in aged hearts. Biochim Biophys Acta Mol Basis Dis *1866*, 165899. 10.1016/j.bbadis.2020.165899.
39. Chan, C.M., Huang, D.Y., Huang, Y.P., Hsu, S.H., Kang, L.Y., Shen, C.M., and Lin, W.W. (2016). Methylglyoxal induces cell death through endoplasmic reticulum stress-associated ROS production and mitochondrial dysfunction. J Cell Mol Med *20*, 1749-1760. 10.1111/jcmm.12893.
40. Senft, D., and Ronai, Z.A. (2015). UPR, autophagy, and mitochondria crosstalk underlies the ER stress response. Trends Biochem Sci *40*, 141-148. 10.1016/j.tibs.2015.01.002.
41. Matsumoto, H., Miyazaki, S., Matsuyama, S., Takeda, M., Kawano, M., Nakagawa, H., Nishimura, K., and Matsuo, S. (2013). Selection of autophagy or apoptosis in cells exposed to ER-stress depends on ATF4 expression pattern with or without CHOP expression. Biol Open *2*, 1084-1090. 10.1242/bio.20135033.

Figure 1. Differential activation of ER stress markers after chronic ER stress in normal human corneal endothelium cell line 21T versus Fuchs' cell line (F35T), primary human corneal endothelial cells, and human corneal tissues. (A) Representative immunoblot data showing differential activation of ER stress-related proteins (eIF2α, p-eIF2α, CHOP, and ATF4) in 21T and F35T cell lines under DMSO (0.2%) and Tun (10 ug/mL) for 24 hours; DMSO was used as solvent control, (B) Immunostaining images ATF4 (green) and mitochondria (labeled with mitotracker red) in F35T and 21T cell lines under normal physiological conditions, (C) Quantification of immunostaining data showing increased % of cells with ATF4 induction in F35T compared to 21T cell line under normal physiological conditions (n = 5, **P < 0.01, unpaired t-test), (D) Immunostaining images showing ATF4 and cytochrome c activation after treatment with Tun (10 ug/24h) in primary human corneal endothelial cells, and (E) Immunostaining showing ATF4 and CHOP induction after treatment with tunicamycin (10 ug/ml, 24 hrs) in human corneal tissues. (scale bar: 20 μm).

Figure 2. Differential Mitochondrial dysfunction induced by ER stress in 21T versus Fuchs' cell line (F35T). (A) Bar graph demonstrating differential MMP loss between 21T and F35T cell lines (0.01, 0.1, 1, and 10 ug/mL Tun), (B) Bar graph demonstrating differences in ATP production between untreated and treated (10 ug/mL Tun) 21T and F35T cell lines; (n = 5, *P < 0.05, **P < 0.01, ***P < 0.001, one-way ANOVA with Tukey's multiple comparison test), (C, D) Representative immunostaining and quantification showing increased mitochondrial fragmentation observed by the release of cytochrome C (red) from mitochondria in F35T compared to 21T cell line after tunicamycin treatment (10 ug/ml at 24h). F35T cell line also has significantly increased mitochondrial fragmentation compared to 21T cell under control (DMSO) at 24 hours (n = 5, *P < 0.05, **P < 0.01, ***P < 0.001, one-way ANOVA with Tukey's multiple comparison test, scale bar: 20 μm), (E) Representative immunoblots showing differential activation of mitochondrial-mediated apoptosis proteins (Bcl2, Cleaved Cas9, Cleaved Cas3, and PARP) in 21T versus F35T cell lines in untreated (0.2% DMSO) and treated (10 ug/mL Tun) conditions at 24 hours (F) Quantification of immunoblot data showing upregulation of pro-apoptotic cleaved PARP, caspase 3 and caspase 9 and downregulation of anti-apoptotic Bcl-2 in F35T cell line compared to 21T cell line under untreated control (n = 5, *P < 0.05, **P < 0.01, unpaired t-test).

Figure 3. Altered mitophagy induced by ER stress in 21T vs F35T cell line. (A) Representative Immunoblot showing differential expression of Mfn2, LC3 A/B, PINK1, and Parkin in 21T and F35T cell lines under untreated and treated condition (0.2% DMSO and 10 ug/ml Tun) at 24 hours, (B) Quantification of immunoblots showing upregulation of parkin and LC3 A/B, and downregulation of PINK1 and Mfn2 in F35T cell line compared to 21T cell line under no treatment (n = 5, *P < 0.05, unpaired t-test), (C) Immunostained images showing increased Parkin activation (green) and cytochrome C release (red) after treatment with tunicamycin (20 ug/mL for 6 h) in 21T cell line (scale bar: 20 μm), (D) Quantification of immunostaining data showing % parkin induction in cells with fragmented mitochondria post tunicamycin treatment (20 ug/mL for 6 h) compared to DMSO, (n = 5, **P < 0.01, unpaired t-test), (E) TEM images showing swollen, fragmented mitochondria and more vacuoles in F35T comapred to 21T cell line under untreated and treated conditions (10 ug/mL Tun for 24 h). Red-colored insets show enlarged images below for better visualization (scale bar: 1 μm).

Figure 4. ATF4 knockdown attenuates ER stress and mitophagy proteins as well as decreases apoptosis under chronic ER stress (A) Western blots showing upregulation of pro-apoptotic ER stress proteins (ATF4, CHOP), mitophagy markers (increaed Parkin and decreased PINK1) and apoptotic proteins (cleaved caspase 3, cleaved caspase 9) and downregulation of mitochondria mass related proteins (Mfn2, Tim23) in tunicamycin treated groups (10 ug/mL, 24h) compared to DMSO (0.2%, 24 hours) under control siRNA and reversal of these ER, mitochondrial, mitophagy and apoptosis markers expression in ATF4-knockdown groups, compared to control siRNA under Tunicamycin (B) Bar graph demonstrating MMP loss post tunicamycin treatment (10 ug/mL Tun) comapred to DMSO (0.2%) under control siRNA at 48 hours in primary corneal endothelial cells while ATF4 knockdown rescues MMP loss compared to control siRNA under Tun (C) Bar graph demonstrating loss of cell viability post tunicamycin treatment (10 ug/mL Tun) compared to DMSO under control siRNA and rescue of cell death post ATF4 siRNA treatment compared to control siRNA under Tun in primary corneal endothelial cells at 24 hours; (n = 5, *P < 0.05, **P < 0.01, ***P < 0.001, one-way ANOVA with Tukey's multiple comparison test), (D) Immunostaining for ATF4 (green) and cytochrome c (red), DAPI (blue) in primary human corneal endothelial cells for control and ATF4 siRNA under DMSO (0.2%) and Tun(10ug/ml) at 24 hours (scale bar: 20 μm), (E) Quantification of immunostaining data showing significant increase in % of fragmented mitochondria post

tunicamycin treatment compared to DMSO under control siRNA and rescue of mitochondrial fragmentation under ATF4 siRNA comparfed to control siRNA under Tun (n = 5, *P < 0.05, **P < 0.01, one-way ANOVA with Tukey's multiple comparison test).

Figure 5. ATF4 knockdown reverses parkin mediated mitophagy and mTOR-AKT-AMPK-mediated autophagy activation under chronic ER stress (A) Immunoblot data from isolated mitochondrial fraction of 21T cells showing increased expression of ATF4, mitophagy mediators Parkin and LC3 and decreased expression of PINK1 post ER stress (0.1 ug/mL Tun at 24 hours) under control siRNA, and decreased expression of mitophagy markers under ATF4 siRNA compared to control siRNA post Tun, (B) Representative immunoblot showing activation of autophagy markers (P-mTOR, P-Akt, P-AMPKα and LC3 A/B) post Tun under ATF4 and control siRNA, (C) Quantification of immunoblots for autophagy markers showing significant upregulation of P-mTOR, P-Akt, and downregulation of P-AMPKα and LC3 A/B under ATF4 siRNA compared to control siRNA post ER stress induction (10 ug/mL Tun at 24h), (n = 5, *P < 0.05, **P < 0.01, one-way ANOVA with Tukey's multiple comparison test), (D,E) TEM images showing mitochondrial swelling and fragmentation, with autophagosomes formation post ER stress induction (10 ug/mL Tun) compared to DMSO (0.2%) at 24 hours while ATF4 knockdown group showed intact and normal ER and mitochondria with no autophagomes compared to control siRNA under Tun (scale bar: 1 μm).

Figure 6. Genetic deletion of ATF4 decreases pro-apototic ER stress molecule, CHOP and protects against UVA-induced cell death. (A) Represntative Zonula occludens-1 (ZO-1, green) immunostaining showing enlargement and loss of corneal endothelial cells (CEnCs) in *ATF4+/+* compared to ATF4+/- mice at week 4 post-UVA (500 J/cm2). (B) Bar graph representing significant decrease in CEnC count in ATF4+/+ compard to ATF4+/- mice post-UVA. (C) Representative immunostained images for CHOP (green) in ATF4+/+ and ATF4+/- mice CEnCs at day 1 post-UVA. (D) Bar graph demonstratting a significant increase in % cells with CHOP in ATF4+/+ compared to ATF4+/- mice post-UVA (n = 5, **P < 0.01, ***P < 0.001, ****P < 0.0001 one-way ANOVA with Tukey's multiple comparison test) (UVA: 500J/cm^2, Scale bar: 20 uM).

Figure 1.

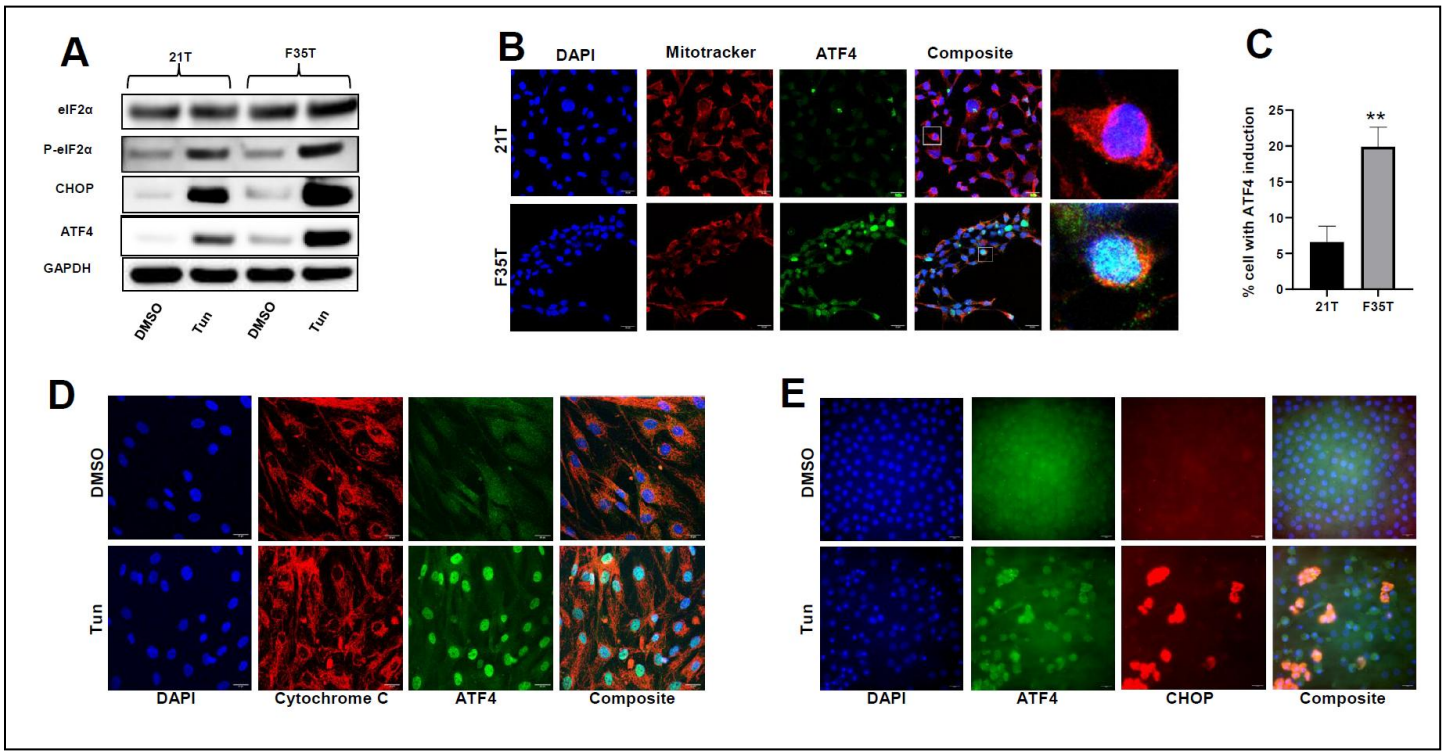
A
21T
F35T
eIF2α
P-eIF2α
CHOP
ATF4
GAPDH
DMSO
Tun
DMSO
Tun
B
DAPI
Mitotracker
ATF4
Composite
21T
F35T
C
% cell with ATF4 induction
25
20
15
10
5
0
**
21T
F35T
D
DMSO
Tun
DAPI
Cytochrome C
ATF4
Composite
E
DMSO
Tun
DAPI
ATF4
CHOP
Composite

Figure 2.

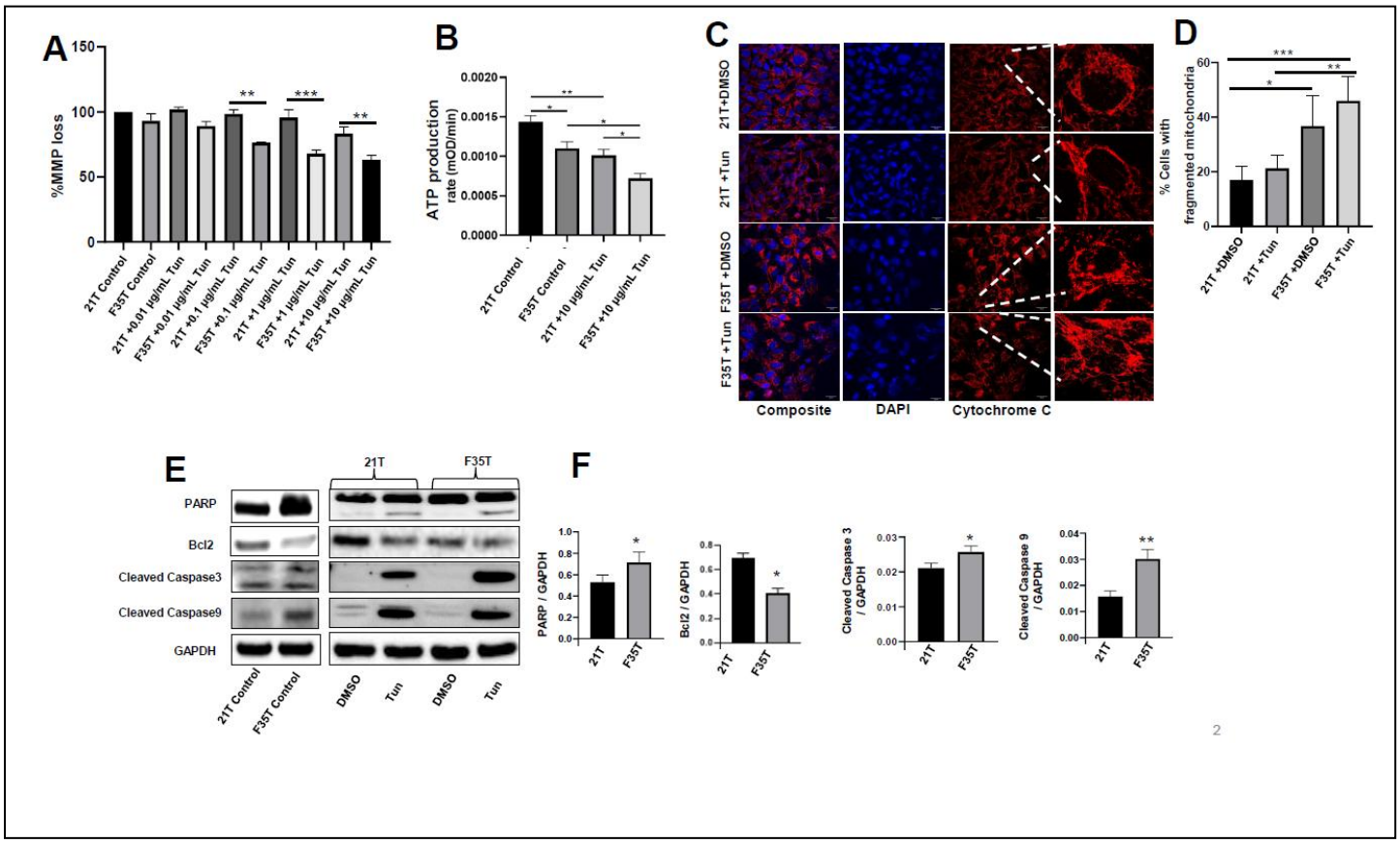
A
%MMP loss
21T Control
F35T Control
21T +0.01 µg/mL Tun
F35T +0.01 µg/mL Tun
21T +0.1 µg/mL Tun
F35T +0.1 µg/mL Tun
21T +1 µg/mL Tun
F35T +1 µg/mL Tun
21T +10 µg/mL Tun
F35T +10 µg/mL Tun
B
ATP production rate (mOD/min)
C
21T+DMSO
21T +Tun
F35T +DMSO
F35T +Tun
Composite
DAPI
Cytochrome C
D
% Cells with fragmented mitochondria
21T +DMSO
21T +Tun
F35T +DMSO
F35T +Tun
E
21T
F35T
PARP
Bcl2
Cleaved Caspase3
Cleaved Caspase9
GAPDH
21T Control
F35T Control
DMSO
Tun
DMSO
Tun
F
PARP / GAPDH
Bcl2 / GAPDH
Cleaved Caspase 3 / GAPDH
Cleaved Caspase 9 / GAPDH
21T
F35T
2

Figure 3.

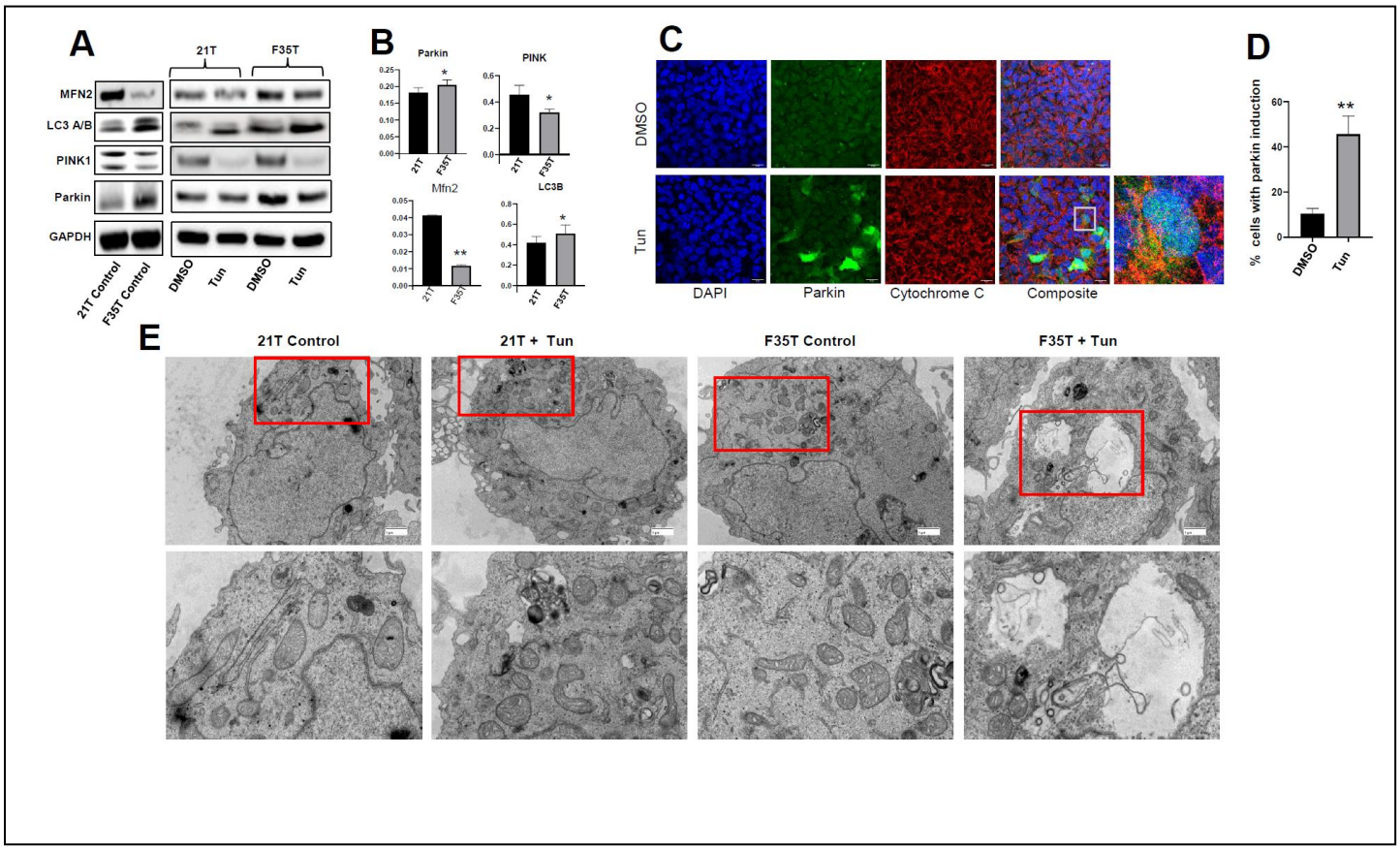
A
21T
F35T
MFN2
LC3 A/B
PINK1
Parkin
GAPDH
21T Control
F35T Control
DMSO
Tun
DMSO
Tun
B
Parkin
PINK
Mfn2
LC3B
21T
F35T
C
DMSO
Tun
DAPI
Parkin
Cytochrome C
Composite
D
% cells with parkin induction
DMSO
Tun
E
21T Control
21T + Tun
F35T Control
F35T + Tun

Figure 4.

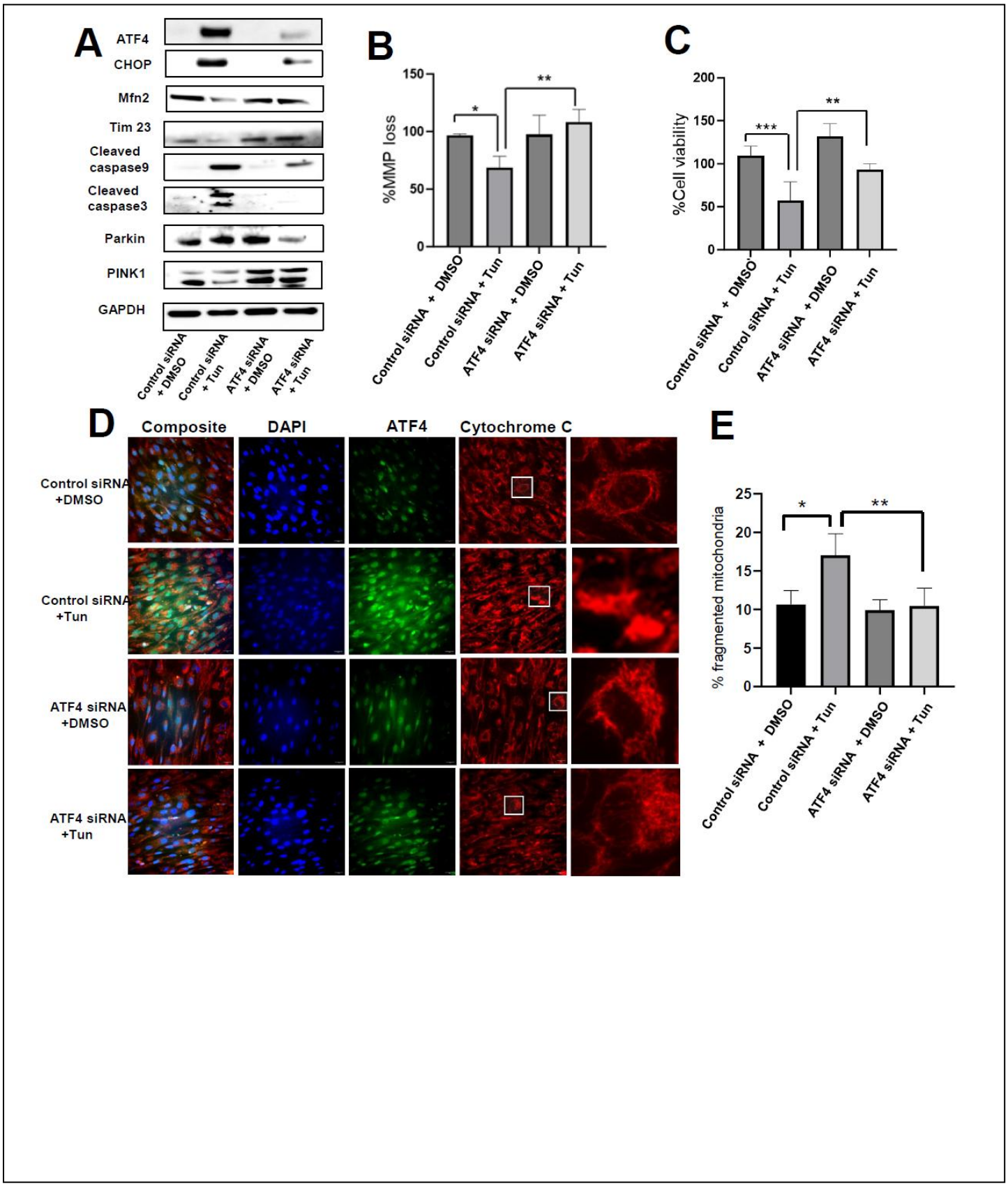
A
ATF4
CHOP
Mfn2
Tim 23
Cleaved caspase9
Cleaved caspase3
Parkin
PINK1
GAPDH
Control siRNA + DMSO
Control siRNA + Tun
ATF4 siRNA + DMSO
ATF4 siRNA + Tun
B
%MMP loss
150
100
50
0
*
**
Control siRNA + DMSO
Control siRNA + Tun
ATF4 siRNA + DMSO
ATF4 siRNA + Tun
C
%Cell viability
200
150
100
50
0
***
**
Control siRNA + DMSO
Control siRNA + Tun
ATF4 siRNA + DMSO
ATF4 siRNA + Tun
D
Composite
DAPI
ATF4
Cytochrome C
Control siRNA +DMSO
Control siRNA +Tun
ATF4 siRNA +DMSO
ATF4 siRNA +Tun
E
% fragmented mitochondria
25
20
15
10
5
0
*
**
Control siRNA + DMSO
Control siRNA + Tun
ATF4 siRNA + DMSO
ATF4 siRNA + Tun

Figure 5.

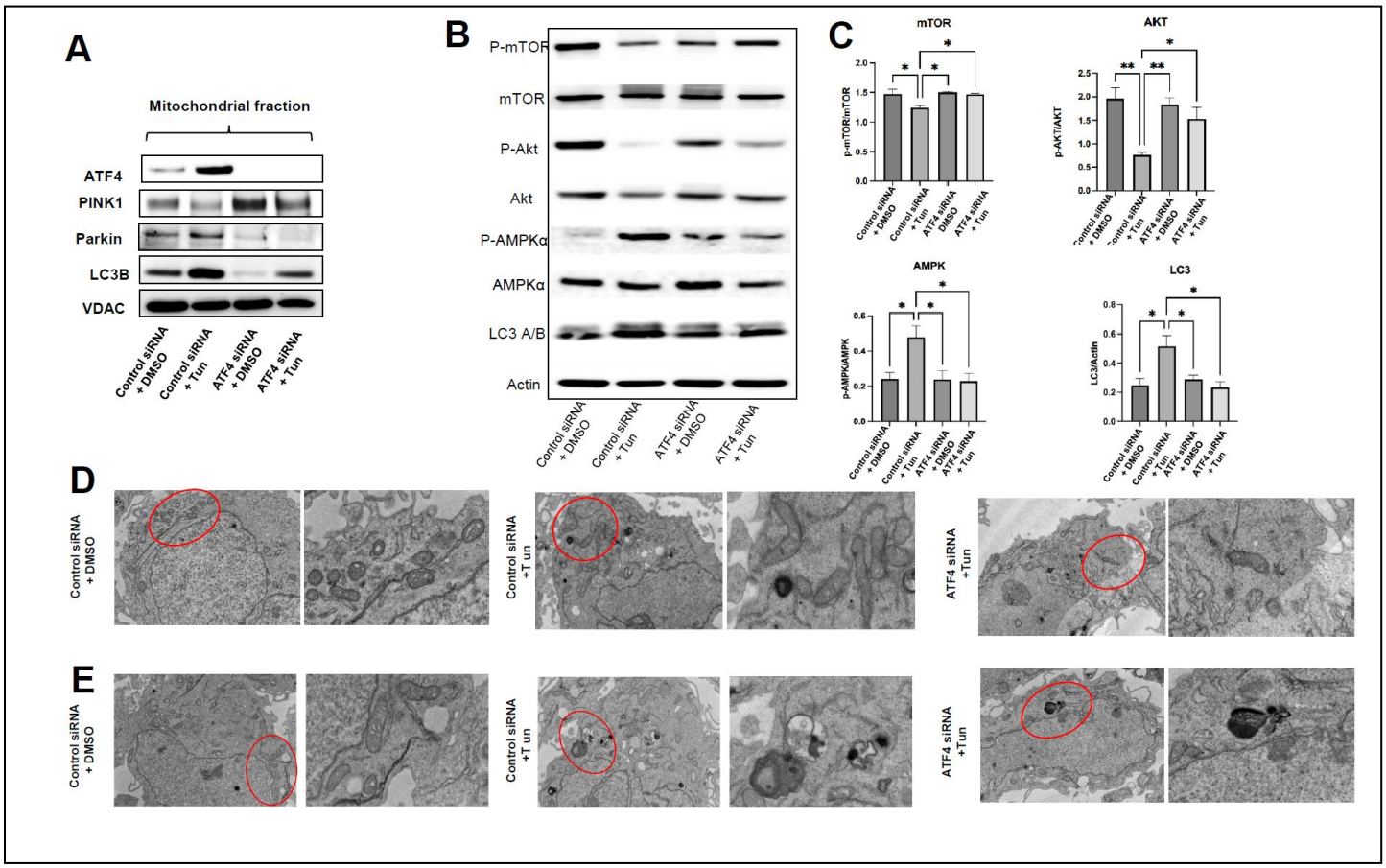
A
Mitochondrial fraction
ATF4
PINK1
Parkin
LC3B
VDAC
Control siRNA + DMSO
Control siRNA + Tun
ATF4 siRNA + DMSO
ATF4 siRNA + Tun
B
P-mTOR
mTOR
P-Akt
Akt
P-AMPKα
AMPKα
LC3 A/B
Actin
C
mTOR
p-mTOR/mTOR
AKT
p-AKT/AKT
AMPK
p-AMPK/AMPK
LC3
LC3/Actin
D
E

Figure 6.

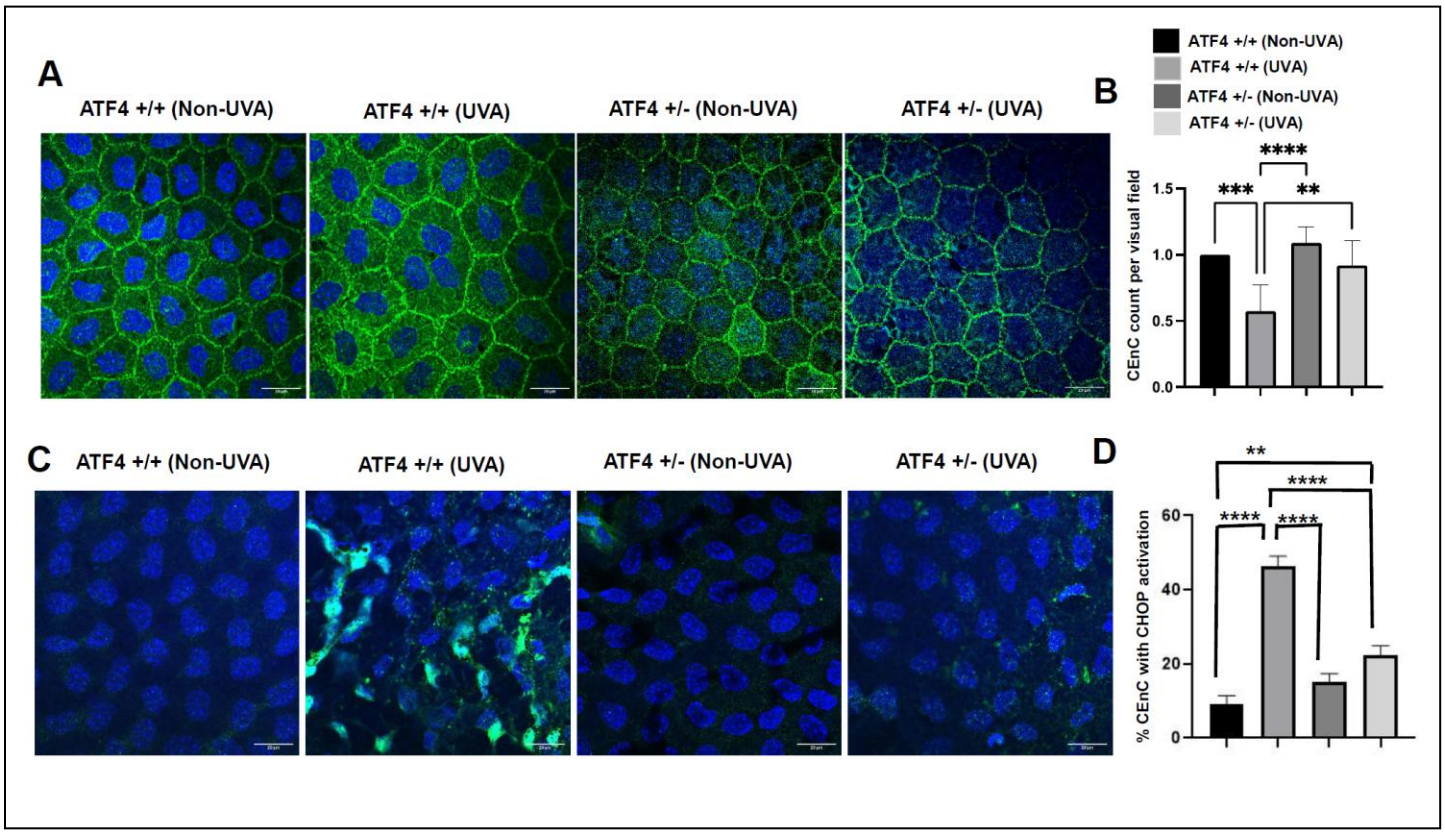
A
ATF4 +/+ (Non-UVA)
ATF4 +/+ (UVA)
ATF4 +/- (Non-UVA)
ATF4 +/- (UVA)
B
ATF4 +/+ (Non-UVA)
ATF4 +/+ (UVA)
ATF4 +/- (Non-UVA)
ATF4 +/- (UVA)
CEnC count per visual field
1.5
1.0
0.5
0.0
***
****
**
C
ATF4 +/+ (Non-UVA)
ATF4 +/+ (UVA)
ATF4 +/- (Non-UVA)
ATF4 +/- (UVA)
D
% CEnC with CHOP activation
60
40
20
0
**
****
****
****